Reduction Mechanism Investigation of Some Schiff Base Podand Derivatives at Glassy Carbon Electrode by Using Electrochemical Techniques

Aybüke A. İsbir-Turan[a], Ali Osman Solak[b], Amgalan Natsagdorj[c], Selen Bilge Koçak[d], Zeynel Kılıç[e]

[a]Ankara University, Faculty of Science, Department of Chemistry, 06100, Tandoğan, Ankara, Turkey, aybuke.turan@gmail.com
[b]Ankara University, Faculty of Science, Department of Chemistry, 06100, Tandoğan, Ankara, Turkey
Kyrgyz-Turk Manas University, Faculty of Eng., Department of Chem. Eng., Bishkek, Kyrgyzstan, aliosman.solak@gmail.com
[c]National University of Mongolia, Department of Chemistry, 210646, Ulaanbaatar, POB-522, Mongolia, anycoj@yahoo.com
[d]Ankara University, Faculty of Science, Department of Chemistry, 06100, Tandoğan, Ankara, Turkey, selenbilge@yahoo.com
[e]Ankara University, Faculty of Science, Department of Chemistry, 06100, Tandoğan, Ankara, Turkey,
zeynel.kilic@science.ankara.edu.tr

Abstract Electrochemical reduction mechanism of some salicylaldimine podands derived from salicylaldehyde and diamines having general formula of $HO-C_6H_4-CH=N-R-N=CH-C_6H_4-OH$ [$R = -, (CH_2)_6, (CH_2CH_2)_2NH, (CH_2CH_2OCH_2)_2$], namely N,N'-bis(salicylidene)-diamine (BSA), N,N'-bis(salicylidene)-1,6-hexanediamine (BSH), 1,7-bis(2-hydroxybenzyl)-1,4,7-triazaheptane (BST), 1,10-bis(2-hydroxybenzyl)-4,7-dioxa–1,10-diazadecane (BDD), respectively, were investigated by using various electrochemical techniques in 0.1 M tetrabutylammonium tetrafluoroborate (TBATFB) in acetonitrile (MeCN) at a glassy carbon (GC) electrode. Schiff base podand derivatives show cyclic voltammetric (CV) irreversible one-electron reduction peaks at about -1.82 V, -2.20 V, -2.14 V and -2.10 V at a scan rate of 0.1 V/s at GC electrode (vs. Ag/Ag$^+$), respectively. The reaction mechanism was investigated by CV and decided to be electrochemical-chemical (*EC*) route and this mechanism was verified by digital simulation. The number of electrons transferred (*n*) and diffusion coefficients (*D*) of the compounds were determined using an ultramicroelectrode (UME) by CV, chronoamperometry (CA) and hydrodynamic voltammetry.

Keywords: *Podand, digital simulation, EC mechanism, cyclic voltammetry, hydrodynamic voltammetry*

Özet $HO-C_6H_4-CH=N-R-N=CH-C_6H_4-OH$ [$R = -, (CH_2)_6, (CH_2CH_2)_2NH, (CH_2CH_2OCH_2)_2$], adlandırması N,N'-bis(salisiliden)-diamin (BSA), N,N'-bis(salisiliden)-1,6-hekzandiamin (BSH), 1,7-bis(2-hidroksilbenzil)-1,4,7-triazaheptan (BST), 1,10-bis(2-hidroksibenzil)-4,7-dioxa–1,10-diazadekan (BDD) olan salisilaldehit ve diaminlerden sentezlenen bazı salisilaldimin podandların bazı elektrokimyasal tekniklerle asetonitrilde hazırlanmış 0,1 M tetrabutilamonyum tetrafloroborat (TBATFB) ortamında ve camsı karbon elektrot kullanılarak elektrokimyasal indirgenme mekanizması araştırılmıştır. Dönüşümlü voltametri tekniği kullanılarak 0.1 V tarama hızında (Ag/Ag$^+$ yardımcı elektrot kullanılarak) ve camsı karbon elektrotta Schiff baz türevlerine ait tersinmez bir elektronlu indirgenme pikleri sırasıyla, yaklaşık olarak -1.82 V, -2.20 V, -2.14 V ve -2.10 V olarak bulunmuştur. Reaksiyon mekanizmaları EC olduğuna karar verilmiş ve EC mekanizması dijital simülasyon ile kanıtlanmıştır. Bileşiklerin elektron aktarım sayısı (n) ve difüzyon katsayısı (D); ultramikroelektrot kullanılarak, dönüşümlü voltametri (CV), kronoamperometri (CA) ve hidrodinamik voltametri teknikleri ile elde edilmiştir.

Anahtar Sözcükler *podand, dijital simülasyon, EC mekanizması, dönüşümlü voltametri, hidrodinamik voltametri*

1. INTRODUCTION

Podand is the family name given to acylic polyethers which have been widely used as host type molecules in metal complex formations [1] and supramolecular chemistry [2]. Over the past 25 years, extensive research has surrounded the synthesis and use of salicylaldimine podands which are the condensation products of salysilaldehyde and amines. This is originated from the fact that the salicylaldimine podands and their metal complexes exhibit wide applications [3-9], especially in biological systems including antibacterial [10,11], antifungal [12], anticancer [13] and herbicidal [14] activities. Recent publications show increased attention to podand type compounds as corrosion inhibitors in especially acidic environments for various metals such as steel, aluminium and copper [15,16]. The use of some salicylaldimine podands in the construction of PVC-based membrane selective sensors for some transition metal ions have also been an area of interest in chemistry [17-19]. In addition, their complexes have important contribution in the development of catalysis [20]. Since salicylaldimine podands exhibit good luminescent properties [21,22] and remarkable photochromic and thermochromic behaviors [23-27] as a consequence of intramolecular proton transfer between phenolic oxygen and imine nitrogen sites in the six-membered chelate ring formed, much work has been devoted in the last few years to the physicochemical characterization of these compounds. In view of the importance of this class of compounds, our group has focused on the synthesis and structural investigations of salicylaldimine podands derived from salicylaldehyde and various diamines and intramolecular hydrogen bonds and tautomerism in these compounds [28-30].

In the present work, we investigated the electroreduction of four Schiff base podand derivatives which represents potential tetradentate salicylaldimine Schiff bases, namely N,N'-bis(salicylidene)-diamine (BSA), N,N'-bis(salicylidene)-1,6-hexanediamin (BSH), 1,7-bis(2-hydroxybenzyl)-1,4,7-triazaheptane (BST), 1,10-bis(2-hydroxybenzyl)-4,7-dioxa–1,10-diazadecane (BDD) at the glassy carbon (GC) electrode in acetonitrile. The mechanism of the electrochemical reduction and the kinetics for the electron transfer of some Schiff base podands was determined with cyclic voltammetry, chronoamperometry and hydrodynamic voltammetry.
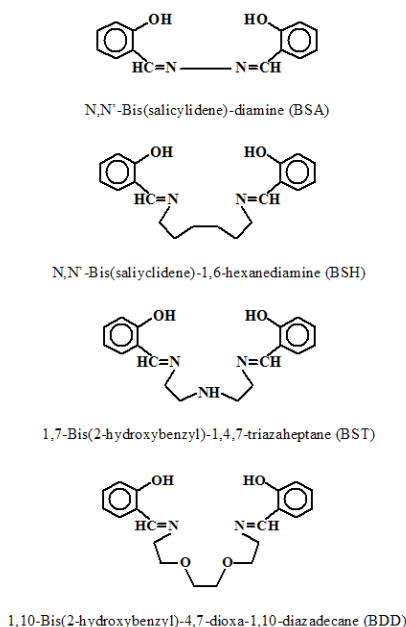
2. EXPERIMENTAL SECTION

2.1. Reagents and Chemicals

All preparations of the aqueous solutions, cleaning of the glassware and the polishing of the electrodes were carried out using ultra pure water with a resistance of 18.3 MΩ cm (Human Power I$^+$ Scholar purification system). Chemicals, acetonitrile (MeCN) (Riedel), isopropyl alcohol (IPA) (Riedel), AgNO$_3$ (Fluka), activated carbon (Sigma-Aldrich), tetrabutyl-ammoniumtetrafluoroborate (TBATFB) (Fluka) and ferrocene (Sigma), salicylaldehyde (Fluka), hydrazine hydrate (Merck), hexane-1,6-diamine (Merck), diethylenetriamine (Merk) and 3,6-dioxa-1,8-diaminooctane (Acros) were of reagent grade and used without further purification. BSA [31], BSH [32], BST [33] and BDD [34] podands were synthesized according to the method reported in the literature. Solutions were deaerated by purging using pure argon gas (99.999 %) for 10 minutes prior to the electrochemical experiments. An argon blanket was maintained over the solutions to supply an inert atmosphere during voltammetric measurements. All electrochemical experiments were performed at room temperature.

Thin layer chromatography (TLC) was performed to investigate the final products of the electrochemical reduction. Before TLC experiments, bulk electrolysis (BE) was performed with the solution of BSH podand. The resulting solution of the bulk electrolysis was evaporated to dryness to remove the solvent. The residue was dissolved in toluene:petroleum ether:ethanol:triethylamine (10:50:5:0.5) mixture of (Isse et al. 1997) and subjected to TLC separation.

2.2. Syntheses of the Schiff base podand derivatives

Salicylaldimine podands, BSA, BSH, BST and BDD have been obtained from the reaction of salicyaldehyde and hydrazine monohydrate [31], hexane-1,6-diamine [32], 3,6-dioxa-1,8-diaminooctane [34], respectively, in MeOH and diethylenetriamine in MeCN [33] according to the method reported in the literature given in paranthesis. The structural formula of these podand type molecules are shown in Scheme1.

N,N'-Bis(salicylidene)-diamine (BSA)

N,N'-Bis(saliyclidene)-1,6-hexanediamine (BSH)

1,7-Bis(2-hydroxybenzyl)-1,4,7-triazaheptane (BST)

1,10-Bis(2-hydroxybenzyl)-4,7-dioxa-1,10-diazadecane (BDD)

Scheme 1. Structural formula, general and short names of the Schiff base podand derivatives.

2.3. Instrumentation

A conventional three-electrode electrochemical system was used for all electrochemical experiments. Ag/Ag$^+$ (0.01 M AgNO$_3$) in MeCN (0.1 M TBATFB) reference electrode and a Pt wire counter electrode were used in all voltammetric measurements. To prepare the Ag/Ag$^+$ (0.01 M AgNO$_3$) reference electrode, pure solid AgNO$_3$ was dissolved in 0.1 M TBATFB in MeCN to obtain a 0.01 M Ag$^+$ inner solution and this electrode was calibrated against ferrocene and checked monthly for its potential. BAS Model MF-2012 GC electrodes with a geometric area (A) of 0.071 cm^2 were used to investigate the electrochemical behavior of the Schiff base podand derivatives. BAS Model 10 µm MF-2007 GC UME was used for the determination of number of electrons transferred. BAS Model MF-2066 rotating disc GC electrode was used in hydrodynamic voltammetric experiments. Experiments of cyclic voltammetry, chronoamperometry and hydrodynamic voltammetry were carried out using a CV-50W electrochemical analyzer (Bioanalytical Systems, West Lafayette, IN, USA) equipped with a BAS C3 Cell Stand.

2.4. Glassy carbon electrode preparation

GC electrodes were prepared by polishing to get a mirror-like appearance, first with fine wet emery papers (grain size 4000) and then with 0.3 µm and 0.05 µm alumina slurry on micro cloth pads (Buhler, USA). First, GC electrodes were sonicated in the water twice and then in 1:1 (v/v) isopropyl alcohol and acetonitrile mixture (IPA+MeCN) to eliminate the alumina dust residues.

IPA and MeCN were separately treated with an equal volume of Norit A activated carbon for 10 min. each, to eliminate the organic impurities.

3. DISCUSSIONS and CONCLUSIONS

3.1. Electrochemical reduction of some Schiff base podand derivatives

Electrochemical reduction of some Schiff base podand derivatives on glassy carbon electrode have been investigated by using cyclic voltammetry and hydrodynamic voltammetry techniques. Cyclic voltammetry technique is especially used to characterize the surface electrochemistry of the electrode material and the mechanism of the number of electrons transferred of the system. Hydrodynamic voltammetry technique is also used to characterize the number of electrons transferred. In this study the current-potential curves of 1 mM solutions of some Schiff base podand derivatives are given in Fig. 1(a-d).
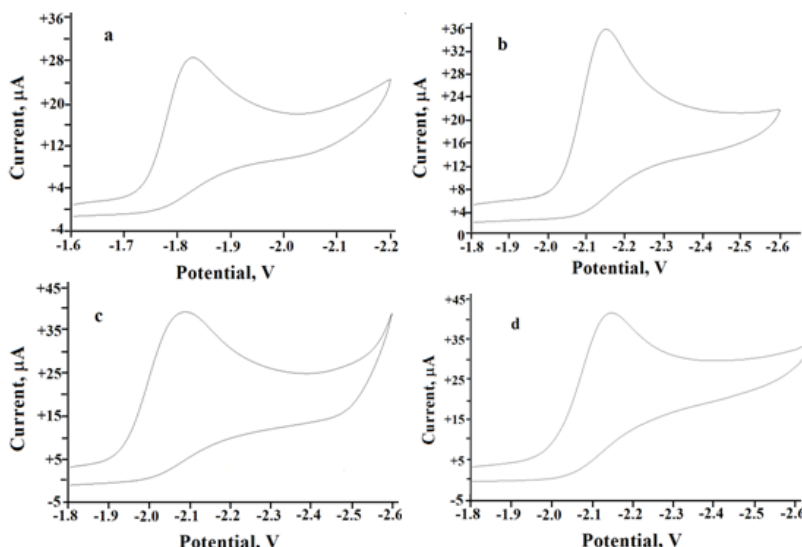
Figure 1. *i-E* curve for 1 mM solution of (a) BSA (b) BSH (c) BST (d) BDD Schiff base podand derivatives in 0.1 M TBATFB in MeCN.

Voltammetric behavior of BSA, BSH, BST and BDD in MeCN (0.1 M TBATFB) are featured by a single reduction peak at a GC surface. Peak potentials and peak currents of the Schiff base podand derivatives are given with their standard deviation for four CV experiments in Table 1. These values are at about -1.82 V, -2.20 V, -2.10 V and -2.10 V at a scan rate $v = 0.1$ V/s.

Table 1. Cyclic voltammetric peak potentials and currents of the Schiff base podand derivatives (1 mM each).

| Compound	$-E_p$ (V)	$i_p (10^5)$(A)
BSA	1.82	2.26
BSH	2.20	2.80
BST	2.14	3.31
BDD	2.10	2.36

* Standard deviations for four measurements.

On the other hand, no anionic peak was observed. It means that, the charge transfer reaction of adsorbed protonated species on the electrode surface is irreversible. Thus, each of these peaks

corresponds to a one-electron irreversible reduction as shown in Fig. 1(a-d). The electrode reaction mechanism of the Schiff base podand derivatives seems to be EC or ECEC type up to the switching potentials, as will be discussed later.

3.2. Determination of the n and D values

Baranski et al. investigate to determine the n and D values in their articles (Baranski, Fawcett and Gilbert 1985). Due to this article, CA and CV experiments were achieved at a conventional GC electrode and a GC ultramicroelectrode for 1 mM of the podand derivatives, respectively. Ferrocene solution (1 mM) was used as reference solution in CV experiments for determination of n according to the method developed by Baranski et al. [35]. Steady-state voltammograms at the UME for ferrocene and the podand derivatives are shown in Fig. 2(a-e).
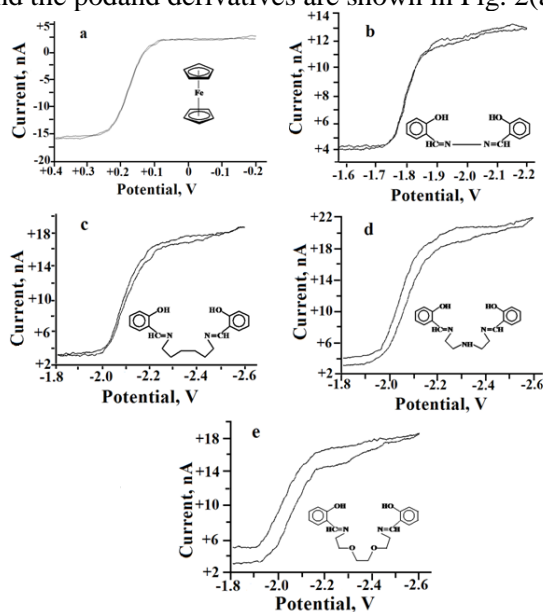
Figure 2. Cyclic voltammetric experiments that carried out at a GC ultramicroelectrode for 1 mM solution of (a) ferrocene (b) BSA (c) BSH (d) BST (e) BDD.

Also, n and D values were calculated by using Equation 1 and Equation 2; where S is the slope of the Cottrell plot, i is the steady-state current (A), C is the concentration (mol/cm^3) for the Schiff base podand derivatives. i_S, C_S and S_S are the same terms but the standard system values for ferrocene.

$$n = \frac{n_S S^2 i_S C_S}{S_S^2 i C} \tag{1}$$

$$D = \frac{D_S S_S^2 i^2}{S^2 i_S^2} \tag{2}$$

All of the terms of the Cottrell slopes, steady-state currents, n and D values for the Schiff base podand derivatives and ferrocene determined from the CA and CV studies are shown in Table 2. As can be seen in Table 2, the number of electrons transferred for the reduction of the Schiff base podand derivatives were calculated as 1.

Table 2. The Cottrell slopes, steady-state currents, n and D values for the Schiff base podand derivatives and ferrocene.

Compound	Cottrell Slopes (S)	UME steady-state currents (i, A)	Numbers of e- transfer	D, cm^2/s
BSA	6.30	1.18	0.9	$(0.48\pm0.07)\times10^{-5}$*
BSH	8.93	1.65	1.3	$(1.88\pm0.62)\times10^{-5}$
BST	7.53	2.05	0.7	$(2.07\pm0.33)\times10^{-5}$
BSD	1.02	1.76	1.4	$(2.85\pm0.37)\times10^{-5}$
Ferrocene	8.15	1.72	1**	$(1.70\pm0.06)\times10^{-5}$

* Standard deviations for four measurements.
**[36]

3.3. Hydrodynamic Voltammetry Measurements

The number of electrons transferred of BSA, BSH, BST and BDD were determined with a rotating disc GC electrode by hydrodynamic voltammetry [36]. Due to the hydrodynamic voltammetry, the solution is stirred by the rotating electrode and the current is measured as the function of the potential applied to a solid working electrode. For 1 mM solution of each Schiff base podand derivatives, all CV experiments were performed with 0.1 V/s scan rate at an angular velocity of 400 rpm. As shown in Fig. 3(a-d) voltammograms of BSA, BSH, BST and BDD were acquired by rotating disc GC electrode to show peak current and potential for the reduction of the podand derivatives.
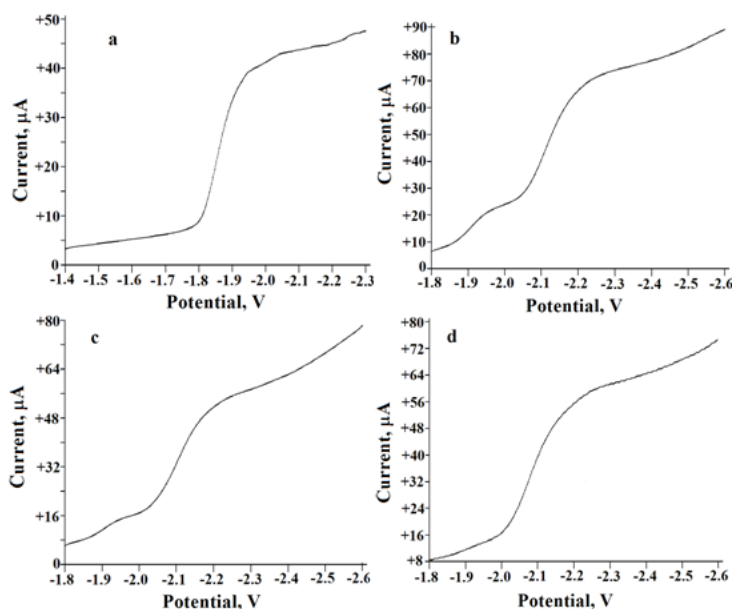
Figure 3. Hydrodynamic voltammograms of 1 mM solution of (a) BSA, (b) BSH, (c) BST, (d) BDD at a scan rate of 0.1 V/s and 400 rpm angular velocity vs. Ag/Ag$^+$ reference electrode.

Furthermore, due to Equation 3, n values were calculated according to the Levich Equation; where i is the peak current (A), F is the Faraday constant, A is the surface area of the electrode (cm^2), C is the concentration of the solution (mol/cm^3), D is the diffusion coefficient, υ is the scan rate (V/s), ω is the angular velocity (s^{-1}).

$$i = 0.62nFACD^{2/3}\upsilon^{-1/6}\omega^{1/2} \tag{3}$$

Using this equation e- transfer number, n was determinate [36]. To determine n, the value of A was used from the ferrocene experiments and it shows the real surface area. Table 3 shows the half wave potential ($E_{1/2}$), steady-state current (i_l), diffusion coefficient (D) and numbers of electron transferred (n) for the Schiff base podand derivatives obtained from the CV and hydrodynamic voltammetry experiments.

Table 3. Half wave potential ($E_{1/2}$), steady-state current (i_l), diffusion coefficient (D) and numbers of electron transferred (n) for the Schiff base podand derivatives.

Compound	$-E_{1/2}$ (V)	$i_l \times 10^5$ (A)	D (cm^2/s)	n
BSA	1.85	4.42	$(0.48\pm0.07)\times10^{-5}$*	1.30
BSH	2.13	5.44	$(1.88\pm0.62)\times10^{-5}$	0.80
BST	2.11	5.10	$(2.07\pm0.33)\times10^{-5}$	0.70
BDD	2.10	4.01	$(2.85\pm0.37)\times10^{-5}$	0.45
Ferrocene	–	6.40	$(1.70\pm0.06)\times10^{-5}$	1**

* Standard deviations for 4 measurements

** [36]

As shown in Table 3, the number of electrons transferred for the reduction of the Schiff base podand derivatives was calculated as one from the rotating disc electrode experiments. Using rotating disc GC electrode, CV voltammograms of BSA, BSH, BST, BDD and ferrocene molecules were taken at 5 different angular velocity as 400, 600, 800, 1000 and 1200 rpm and scan rate of 0.1 V/s. Then, heterogen standard rate constant (k°) and transfer coefficient (α) values for the reduction of the Schiff base podand derivatives in MeCN solution were determined according to the Kotecky-Levich Equation and from the graph of $1/i_l$ vs. $1/(\omega)^{1/2}$ as shown in Table 4.

Table 4. Transfer coefficients and heterogen standard rate constants of podand derivatives.

Compound	α	k°
BSA	0.52	1073
BSH	0.46	1198
BST	0.36	424
BDD	0.26	409

When the n values of the Schiff base podand derivatives that were determined from UME and RDE experiments are compared, it can easily be said that the electrode reaction of the Schiff base podand derivatives occurs through the irreversible one electron reduction mechanism. Comparison of numbers of electrons transferred for the Schiff base podand derivatives were given in Table 5.

Table 5. Comparison of the n values found from the experiments at UME and RDE for the podand derivatives.

| Compound	n (from UME)	n (from RDE)
BSA	0.9	1.3
BSH	1.3	0.8
BST	0.7	0.7
BDD	1.4	0.5
Ferrocene	1*	1*

*[36]

It is shown that the final n values those were determined form the UME and RDE measurements for the Schiff base podand derivatives are approximately closer to each other. This means that, one of the kinetic properties as the number of electrons transferred values (n) for the Schiff base podand derivatives those were 1, was verified by two voltammetry technique and overlapping with each other.

3.4. Electrode reaction mechanisms of the Schiff base podand derivatives at the glassy carbon electrode

For the investigation of mechanism for the electrode reactions of Schiff base podand derivatives at the GC electrode, CV voltammograms of the Schiff base podand derivatives were acquired at different scan rates between 1 V/s and 10 V/s at the same potential ranges. CV voltammograms of the Schiff base podand derivatives are given in Fig. 4.
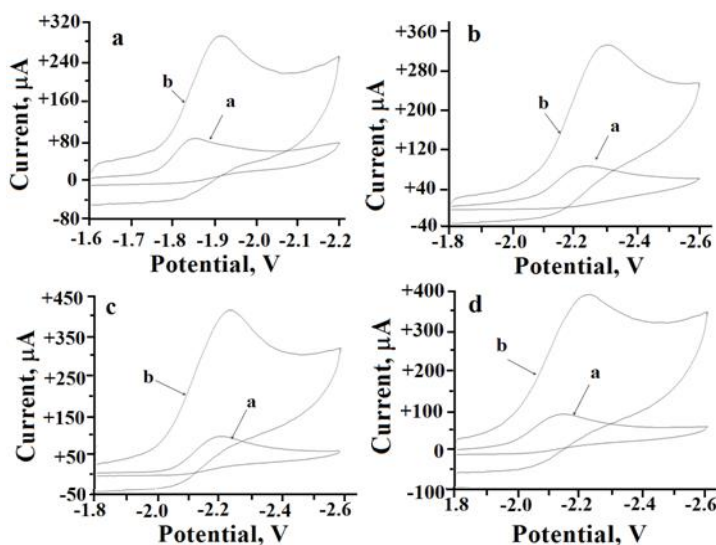

Figure 4. CV voltammograms of 1 mM solution of BSA, BSH, BST and BDD at (a) 1 V/s and (b) 10 V/s vs. Ag/Ag$^+$ reference electrode.

All the Schiff base podand derivatives have one cathodic peak but no anodic peak at the lower scan rates. When the scan rate was increased 10 fold, a small anodic peak appeared in the voltammograms of all derivatives, indicating the presence of a follow up chemical reaction accompanying the electron transfer reaction. The follow up chemical reaction might be a protonation, dimerization or polymerization reaction that uses the reduced podand moieties. To investigate and understand that the homogeneous follow up reaction is a protonation reaction or not, the voltammetric experiments were occured in dry acetonitrile medium [37]. In the end of these voltammetric experiments, it is shown that voltammogram of the Schiff base podand derivatives in dried acetonitrile medium is similar to the one acquired in undried acetonitrile medium and implying that the following chemical reaction is not a protonation reaction.

In the following, Scheme 2 shows the proposed reaction mechanism of the Schiff base podand derivatives.
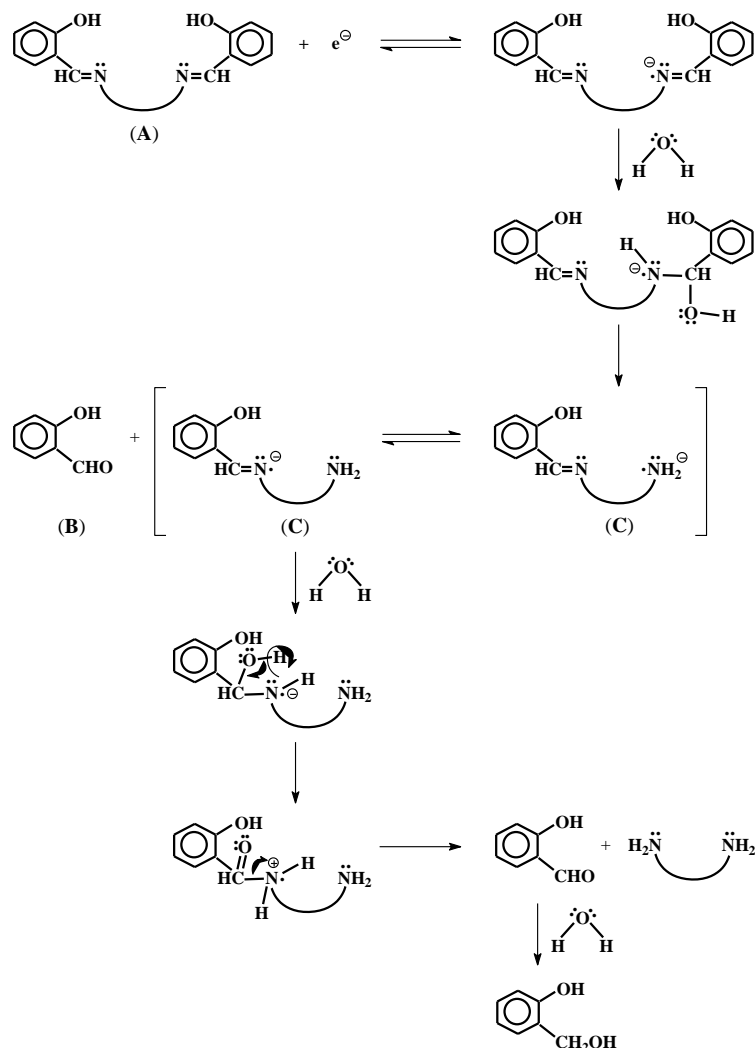
Scheme 2. Schematic representation of the proposed reaction mechanism for the electrochemical reduction of the Schiff base podand derivatives.

According to Scheme 2, podand (A) is reduced to an anion radical with a one electron transfer to the one of the imine groups. Since the anion radical is a very reactive moiety, it is immediately hydrolyzed by the trace amount of the water in acetonitrile. [38]. As a result of this hydrolysis reaction, salicylaldehyde (B) and a Schiff base (C) are produced. The Schiff base product is then converted to the salicylaldehyde and diamine products thorough the hydrolysis reaction, as shown in Scheme 2. To confirm the electrode reaction mechanism, following the bulk electrolysis of BSH podand as a representative compound, the solution is evaporated to dryness to remove the solvent. The residue is dissolved in toluene (0.1) + petroleum ether (0.5) + ethanol (0.05) + triethylamine (0.005) mixture [39] and subjected to TLC seperation. The electrolysis products of BSH podand are detected at TLC with the R_f values of 0.625 for salicylaldehyde; 0.042 for BSH and 0.069 for 2-hydroxybenzyl alcohol.

We used DigiSim[®] 3.03 simulation software to confirm the reaction mechanism and to estimate the kinetic parameters for electrochemical and chemical steps. After establishing the EC mechanism, the appropriate parameter values such as heterogeneous rate constant (k^0),

54

equilibrium constant (K), and forward and backward rate constants (k_f, k_b) of the chemical step were optimized by varying the associated parameter values and following the effects of these parameters on the CV responses. The values of the various parameters are given for the simulation after fitting to the experimental voltammograms in Table 6.

Table 6. Optimized parameters for the electrochemical reduction of Schiff base podand derivatives by comparing the theoretical and experimental voltammograms.

Compound	$k°$ (cm/s)	K	k_f (s^{-1})	k_b (s^{-1})
BSA	≥ 0.85	1×10^3	100	0.1
BSB	≥ 0.95	1×10^3	100	0.1
BSD	≥ 0.95	1×10^3	100	0.1
BDD	≥ 0.80	1×10^3	100	0.1

The final fitted and experimental voltammograms are shown in Fig. 5(a-d). The dotted graphs show the theoretical CV voltammograms while the solid lines show the experimental ones. During the simulation work, the electrode mechanism that was accepted as ECEC and the criteria were chosen suitable for this. On the other hand, nearby the criteria of the ECEC, mechanism of EC was chosen and because of the occurrences of the electrochemical reduction and chemical reaction. Toward this, the Schiff base podand derivative in the medium was given an electrochemical reaction and then given a rapid chemical reaction with the trace amount of the water. At last, Schiff base podand derivative transforms to the products. One of the products namely, salicylaldehyde was reduced to radical form with electrochemical reduction. Then chemically reacted with the trace amount of the water in the medium and another product was occurred in the end. Finally, simulations of the experiment voltammograms were done due to the two of EC mechanism those were occurred following one after another.
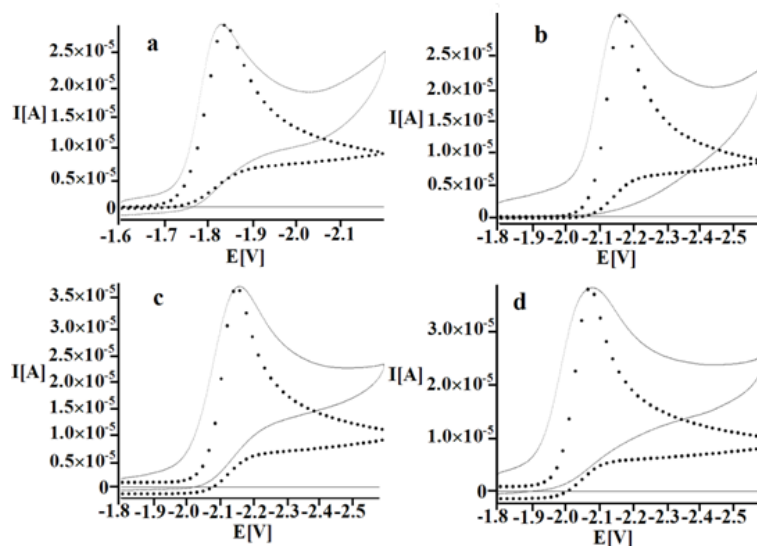
Figure 5. Comparison of the experimental and theoretical CV voltammograms of (a) BSA, (b) BSH, (c) BST, (d) BDD vs. Ag/Ag$^+$ reference electrode at the scan rate of 0,1 V/s.

According to fit of the theoretical and experimental voltammograms above, it is easily seen that the suitability of EC mechanism is more acceptable for the electrode mechanisms of these type Schiff base podand derivatives. In Table 6, the electrons transferred rate constants of the Schiff

base podand derivatives were determined ≥0.6 cm/s. Voltammograms of the Schiff base podand derivatives that were recorded from the experimental studies, especially due to the peak forms and ΔE_p at the low scan rates show that Schiff base podand derivatives have high electrons transferred in acetonitrile medium.

Electrochemical reduction mechanism of the Schiff base podand derivatives were investigated by using various electrochemical techniques at a glassy carbon (GC) electrode. The number of electrons transferred (n) and diffusion coefficients (D) of the compounds were determined using an UME by CV, CA and hydrodynamic voltammetry. The reaction mechanism was investigated by CV, and then two of EC mechanism was verified a following one after another by digital simulation. And the simulations were given well suitability of the experiments and the theoretical voltammograms of the Schiff base podand derivatives.

Acknowledgement

REFERENCES

[1] Boschke EL, (1981). Topics in Current Chemistry, "Host-Guest Complex", Volumes I-III, ed., Springer Verlag, Berlin, , 1982-1984.
[2]   Steed JW, Atwood JL, 2002. Supramolecular Chemistry, Chichester, UK: J. Wiley and Sons.
[3] Holm RH, O'Connor MJ, (1971). The Stereochemistry of Bis-Chelate Metal(II) Complexes. Progresses in Inorganic Chemistry, 14: 241-401.
[4] Costamagna J, Vargas J, Lattorre R, Alvarado A, Mena G, (1992). Coordination Compounds of Copper, Nickel and Iron with Schiff Bases Derived from Hydroxynaphthaldehydes and Salicylaldehydes. Coordination Chemistry Reviews, 119: 67-88.
[5] Garnovskii AD, Nivorozhkin AL, Minkin VI, (1993). Ligand Environment and The Structure of Schiff Base Adducts and Tetracoordinated Metal-Chelates. Coordination Chemistry Reviews, 126: 1-69.
[6] Guerriero P, (1995). From Mononuclear to Polynuclear Macrocyclic or Macroacyclic Complexes. Coordination Chemistry Reviews, 139: 17-243.
[7] Luo H, Franwick PE, Green MA, (1998). Synthesis and Structure of a Novel Cu(II) Complex with a Monoprotic Tetradentate Schiff Base Ligand. Inorganic Chemistry, 37: 1127-1130.
[8] Chen D, Martel AE, (1987). Dioxygen Affinities of Synthetic Cobalt Schiff Base Complexes. Inorganic Chemistry, 26: 1026-1030.
[9] El-Naggar AM, Ahmed FSM, Badie MF, (1981). Synthesis of Some 2-(*N*-Protected or Free Aminoacyl or *N*-tosyltripeptide)-Aminophenazines, Aminonaphthophenazines and 4-(*N*-protected or Free Aminoacyl or *N*-tosyltripeptide)aminophenazone Derivatives**.** Journal of Heterocyclic Chemistry, 18: 91-94.
[10] Karia FD, Parsania PH, (1999). Synthesis, Biological and Thermal Properties of Schiff bases of Bisphenol-C. Asian Journal of Chemistry 11: 991-995.

[11] Cheng K, Zheng Q-Z, Y Qian, Shi L, Zhao J, Zhu H-L, (2009). Synthesis, Antibacterial Activities and Molecular Docking Studies of Peptide and Schiff Bases as Targeted Antibiotics. Bioorganic and Medicinal Chemistry, 17: 7861-7871.

[12] Singh WM, Dash BC, (1988). Synthesis of Some New Schiff Bases Containing Thiazole and Oxazole Nuclei and Their Fungicidal Activity. Pesticides, 22(11): 33-37.

[13] Desai SB, Desai PB, Desai KR, (2001). Synthesis of some Schiff bases, thiazolidones, and azetidinones derived from 2,6-diaminobenzo[1,2-*d*:4,5-*d*']bisthiazole and their anticancer Activities. Heterocyclic Communications, 7:83-90.

[14] Samadhiya S, Halve A, Orient. (2001). Synthetic Utility of Schiff Bases as Potential Herbicidal Agents. Journal of Chemistry, 17: 119-122.

[15] Hasanov R, Bilge S, Bilgiç S, Gece G, Kılıç Z, (2010). Experimental and Theoretical Calculations on Corrosion Inhibition of Steel in 1 M H_2SO_4 by Crown Type Polyethers. Corrosion Science 52(3): 984-990.

[16] Asan A, Kabasakaloğlu M, Işıklan M, Kılıç Z, (2005). Corrosion Inhibition of Brass in Presence of Terdentate Ligands in Chloride Solution. Corrosion Science, 47(6): 1534-1544.

[17] Mashhadizadeh MH, Sheikhshoaie I, (2003). Mercury(II) Ion-selective Polymeric Membrane Sensor Based on a Recently Synthesized Schiff Base. Talanta, 60. 73-80.

[18] Shamspur T, Mashhadizadeh MH, Sheikhshoaie I, (2005), Flame Atomic Absorption Spectrometric Determination of Silver Ion After Preconcentration on Octadecyl Silica Membrane Disk Modified with Bis[5-((4-nitrophenyl)azosalicylaldehyde)] as a New Schiff Base Ligand. Journal of Analytical Atomic Spectroscopy. 18: 1407-1410.

[19] Shamspur T, Mashhadizadeh MH, Sheikhshoaie I, (2005). Flame Atomic Absorption Spectroscopy (FAAS) Determination of Iron(III) After Preconcentration on to Modified Analcime Zeolite with 5-((4-Nitrophenylazo)-*N*-(2ʹ,4ʹ-Dimethoxyphenyl))Salicylaldimine by Column Method. J. Anal. Atom. Spec. 20: 476-478.

[20] Burger MT, Armstrong A, Guarnieri F, McDonald D, Clark Q, Stil W, (1994). Free Energy Calculations in Molecular Design: Predictions by Theory and Reality by Experiment with Enantioselective Podand Ionophores. Journal of American Chemical Society, 94: 3593-3594.

[21] Wang PF, Hong ZR, Xie ZY, Tong SW, Wong O, Lee CS, Wong NB, Hung LS, Lee ST, (2003). A Bis-salicylaldiminato Schiff Base and Its Zinc Complex as New Highly Fluorescent Red Dopants for High Performance Organic Electroluminescence Devices. Chemical Communication, 19(4): 1664-1665.

[22] Yu G, Liu YQ, Song YR, Wu X, Zhu DB, (2001). A New Blue Light-emitting Material. Synthetic Metals, 117: 211-214.

[23] Ziolek, M, Filipczak K, Maciejewski A, (2008). Spectroscopic and Photophysical Properties of Salicylaldehyde Azine (SAA) as a Photochromic Schiff Base Suitable for Heterogeneous Studies. Chemical Physics Letters, 464(4-6): 181-186.

[24] Wang F, Qin L, Fan M, (1993). Transient Absorption Spectra and Photochromic Mechanism of Schiff Bases. Research on Chemical Intermediates, 19(4): 299-306.

[25] Hadjoudis E, Mavridis IM, (2004). Photochromism and Thermochromism of Schiff Bases in the Solid State: Structural Aspects. Chemical Society Reviews, 33: 579-588.

[26] Zhao J, Zhao B, Liu J, Xu W, Wang Z, (2001). Spectroscopy Study on the Photochromism of Schiff Bases *N,Nʹ-bis*(salicylidene)-1,2-diaminoethane and *N,Nʹ-bis*(salicylidene)-1,6-hexanediamine. Spectrochimica Acta A, 57: 149-154.

[27] Chantarasiri N, Tuntulani T, Tongroung P, Seangprasertkit-Magee R, Wannatong W, (2000). New metal-containing epoxy polymers from diglycidyl ether of bisphenol A and tetradentate Schiff base metal complexes. European Polymer Journal, 36: 695-702.

[28] Bilge S, Kılıç Z, Hayvalı Z, Hökelek T, Safran S, (2009) Intramolecular Hydrogen Bonding and Tautomerism in Schiff Bases: Part VI. Syntheses and Structural Investigation of Salicyialdimine and Naphthaldimine Derivatives. Journal of Chemical Sciences, 121(6): 989-1001.

[29] Hökelek T, Bilge S, Demiriz Ş, Özgüç B, Kılıç Z, (2004). 1,3-[Bis(N-2-oxyphenylsalicylydene)]propane. Acta Crystallographica Section C 60: 803-805.

[30] Bilge S, Natsagdorj A, Akduran N, Hökelek T, Kılıç Z, (2002). C-bis-pivot Podands and Lariat Ethers: Synthesis and Spectral Investigations. Structure of 15,21-bis{2-[(hydroxy)(methoxy)phosphoryl]}-2,5,8-trioxa-16,20-diazatricyclo[20.4.0.0^{9,14}]hexacosa-9,11,13,22,24,26(1)-hexaene-water(1/2). Journal of Molecular Structure, 611: 169-178.

[31] Xu X-X, You X-Z, Sun Z-F, (1994). 2,2'-Azinodimethyldiphenol, $C_{14}H_{12}N_2O_2$. Acta Crystallographica Section C, 50: 1169-1171.

[32] Kanthimathi M, Kumar RM, Dhathathreyan A, Nair BU, Ramasami T, (2000). Liquid Crystalline Properties of Schiff-base Ligands: Role of Flexible Methylene Spacer within the Schiff-base Ligand. Molecular Crystal Liquid Crystalline Science and Technology Section C: Molecular Materials, 12(3): 223-226.

[33] Park M, Kim Y, (2000). Schiff Base Receptor for Salicylaldehyde and Barbituric acid. Thin Solid Films, 363: 156-159.

[34] Yu T, Su W, Li W, Hong Z, Hua R, Li M, Chu B, Li B, Zhang Z, Hu ZZ, (2006). Synthesis, Crystal Structure and Electroluminescent Properties of a Schiff Base Zinc Complex. Inorganic Chimica Acta, 359: 2246-2251.

[35] Baranski AS, Fawcett WR, Gilbert CM, (1985). Use of Microelectrodes for the Rapid Determination of the number of Electrons Involved in an Electrode Reaction. Journal of American Chemical Society, 57(1): 166-170.

[36] Bard AJ, Faulkener LR, 2001. Electrochemical Methods, Second Edition, New York, J. Wiley and Sons.

[37] Kirk JR, Page D, Prazak M, Katovic V, (1988). Electrochemical studies of niobium chlorides in superdry acetonitrile: electron-transfer-induced ligand-exchange reactions. Inorganic Chemistry, 27: 1956-1963.

[38] Sawyer DT, Sobkowlak A, Roberts JL, (1995). Journal of Electrochemistry for Chemists, New York Wiley-Interscience Pub. 7: 305.

[39] Isse AA, Gennaro E, Vanello E, (1997). Electrochemical reduction of Schiff base ligands H_2salen and H_2salophen. Electrochimica Acta, 42: 2065-2071.